White-light filaments for multiparameter analysis of cloud microphysics

Riad Bourayou

Teramobile, Institut für Optik und Quantenelektronik, Friedrich Schiller Universität Jena, Max Wien Platz 1, D-07743 Jena, Germany

Guillaume Méjean and Jérôme Kasparian

Teramobile, Laboratoire de Spectrométrie Ionique et Moléculaire, Unité Mixte de Recherche (UMR 5579) Centre National de la Recherche Scientifique, Université Claude Bernard Lyon 1, 43 Boulevard du 11 Novembre 1918, F-69622 Villeurbanne Cedex, France

Miguel Rodriguez

Teramobile, Institut fur Experimentalphysik Freie Universitat Berlin, Arnimallee 14, D-14195 Berlin, Germany

Estelle Salmon and Jin Yu

Teramobile, Laboratoire de Spectrométrie Ionique et Moléculaire, Unité Mixte de Recherche (UMR 5579) Centre National de la Recherche Scientifique, Université Claude Bernard Lyon 1, 43 Boulevard du 11 Novembre 1918, F-69622 Villeurbanne Cedex, France

Holger Lehmann, Bringfried Stecklum, Uwe Laux, Jochen Eislöffel, Alexander Scholz, and Artie P. Hatzes

Thüringer Landessternwarte Tautenburg, Karl Schwarzchild Observatorium, Sternwarte 5, D-07778 Tautenburg, Germany

Roland Sauerbrey

Teramobile, Institut für Optik und Quantenelektronik, Friedrich Schiller Universität Jena, Max Wien Platz 1, D-07743 Jena, Germany

Ludger Wöste

Teramobile, Institut für Experimentalphysik Freie Universität Berlin, Arnimallee 14, D-14195 Berlin, Germany

Jean-Pierre Wolf

Teramobile, Laboratoire de Spectrométrie Ionique et Moléculaire, Unité Mixte de Recherche (UMR 5579) Centre National de la Recherche Scientifique, Université Claude Bernard Lyon 1, 43 Boulevard du 11 Novembre 1918, F-69622 Villeurbanne Cedex, France

Received March 19, 2004; revised manuscript received September 15, 2004; accepted September 21, 2004

We present a lidar technique using femtosecond-terawatt laser pulses to perform a multiparameter analysis of cloud microphysics. Particle size and density within the cloud are deduced from the multispectral multiple scattering pattern of an ultrashort laser pulse. Furthermore, the spectral analysis of the atmospheric transmission of the white-light continuum from the same laser source yields temperature and relative humidity.

OCIS codes: 120.0280, 190.7110, 260.5950, 280.3640, 290.1090.

1. INTRODUCTION

Cloud nucleation and maturation processes play a key role in atmospheric modeling, both in the meteorological and climatological time and space scales.[1] In particular, both the droplet growth within the cloud and their number density have a strong influence on the Earth albedo and precipitation forecast. Their characterization requires continuous measurements of the droplet size distribution within the cloud, with a time resolution on the order of several tens of minutes, compatible with the growth and evaporation rates. Besides delicate airborne or balloon-borne *in situ* sampling, the most promising techniques are multispectral or multiple-field-of-view

(MultiFOV) lidars.[2] These techniques rely on the critical dependence of the Mie scattering efficiency (backscattering and extinction cross sections of the particles) and angular pattern, respectively, with the wavelength and the particle size. Most suited for optically thin clouds where multiple scattering is negligible, multispectral lidars[3,4] use several wavelengths, typically the harmonics of Nd:YAG lasers. Comparing the corresponding lidar returns, one can fit parameters such as the width and the mean size of a predefined size distribution. Hence, this technique requires *a priori* knowledge about the shape of the size distribution as well as the type of the particles themselves. Adding a depolarization channel moreover allows one to distingush between spherical and nonspherical particles.

Optically thick (i.e., dense) clouds, as relevant for precipitation studies, can be better characterized by MultiFOV[5–8] techniques. Here, the multiple-scattering pattern is recorded for several FOV values by masking parts of the detector to select specific ranges of detection angle. The FOV dependence of the signal can be used to gain information about the size distribution. However, the limited number of FOV values as well as the use of one single wavelength can yield only unambiguous particle sizes if the fitting interval is restricted by use of *a priori* knowledge of the cloud of interest. For the improvement of the sensitivity and reliability of the measurements, new remote particle-sizing techniques are required.

The ultimate goal for a full characterization of the cloud microphysics and micrometeorology, e.g. droplet growth, includes knowledge of the thermodynamic parameters of the atmosphere, and especially the relative humidity and temperature, with a reasonable vertical resolution. Balloon-borne radiosondes have limited horizontal and time-resolution coverage, because of the limited amount of balloons that can be launched, and the lack of control over their trajectory. Differential absorbtion lidars have long been developed that provide good quality data, even in airborne[9–12] or spaceborne[4,13–15] conditions. They can measure both water vapor mixing ratio and the temperature profile from the Rayleigh profile across an adiabatic atmospheric model.[16] Alternative to these very-narrow linewidth (0.01 Å) developments, some groups tried to circumvent the vertical gradients in the Doppler shift and the broadening of the measured line[17] by using broadband (several nanometers) laser sources.[18,19] The emitted spectrum in these experiments is limited, however, intrinsically by the laser process to some tens of nanometers. Efforts to accurately measure water vapor in the atmosphere have also been directed towards Raman lidar.[20,21]

Ultrashort lasers could contribute to a better characterization of the cloud microphysics. In the nonlinear propagation of terawatt-femtosecond laser pulses, filamentation[22–25] generates a white-light continuum extending from the ultraviolet[26,27] to the infrared.[28] This directional, broadband emission provides a basis for white-light lidar, i.e. multispectral lidar measurements with high spectral resolutions over a bandwidth of several hundreds of nanometers. White-light lidar was recently demonstrated to allow the simultaneous range-resolved detection of several atmospheric species,[29–33] including the atmospheric water vapor volume mixing ratio (VMR).[30] However, simultaneous temperature measurement could not be achieved together with the water VMR to allow the determination of the relative humidity.

In this paper, we show that the multiple-scattering pattern around the white-light beam impact on the bottom of the cloud can yield a measurement of its droplet size distribution and density. Moreover, high-resolution broadband spectra obtained in the white-light lidar returns by use of the same laser source provide the water vapor VMR and temperature of the atmosphere below the cloud layer, which in turn yield the relative humidity of the atmosphere. Although this demonstration was performed in two successive experiments, these experiments both use the same laser source and could be driven simultaneously, opening the potential for a multiparameter remote characterization of cloud microphysics.

2. EXPERIMENTAL SETUP

The experiments reported in this paper were performed with the mobile femtosecond terawatt laser Teramobile.[34] This chirped-pulse amplification Ti:sapphire-based laser chain delivered 300-mJ pulses centered at 795 nm at a repetition rate of 10 Hz. The minimum pulse duration (Fourier limited) was 70 fs. However, for the measurements presented here, the pulses were slightly negatively chirped in the compressor, i.e. the shorter wavelength (blue) component of the laser pulse, which intrinsically has a 15-nm broad spectrum, was emitted ahead of the redder one, to compensate for the atmospheric group velocity dispersion. Adjustment of the chirp permits us to control the range and the onset position of filamentation.[34] The corresponding initial pulse duration was 150 fs for multiple-scattering measurements and 300 fs for spectral measurements. The terawatt output beam was sent collimated with a diameter of 3 cm.

Contrary to early white-light lidar experiments using flashlamps, or more recent demonstrations where a femtosecond continuum was generated in a nonlinear medium at ground level,[35] our experiment was based on white light generated *in situ* by filaments in the atmosphere. Therefore the light source can be characterized only indirectly by observations from the ground. Four key parameters are the white-light spectrum, its angular distribution (wavelength-dependent divergence), the altitude of the source (filament height), and the backscatter function, including the backward-enhanced white-light emission.[36]

The spectrum can be inferred from ground measurements,[27,28] although it has been recently suggested that at least the conversion efficiency into the white-light continuum may be affected by the generation over long distances in the atmosphere.[32] Moreover, we have measured that the white-light divergence in the same experimental conditions is slightly below 1 mrad,[37] much wider than the 1.2-arcsec FOV of the telescope used in the spectral measurements. Therefore the wavelength dependence of the divergence and the backscatter function distort the observed spectrum, preventing us from considering the spectrum of our white-source to be pre-

cisely known. Nevertheless, it is well known that the continuum spectrum is smooth, whereas we measure narrow absorption lines. This permits us to deconvolve the partly unknown spectrum of the light source, as detailed in Section 4. Also, the filament height can be controlled and adjusted up to several kilometers through adjustment of the initial chirp of the laser.[34,37] However, we cross checked the filament altitude by fitting the oxygen absorption spectrum during some measurements.

The receiving system consisted of the 2-m primary mirror telescope[38] of the Thüringer Landessternwarte observatory (341-m altitude), located 30 m away from the laser. For this demonstration experiment, where no range resolution was sought, the telescope was aimed at the impact of the laser beam on the bottom of the cloud layer, which was imaged on a time-integrating CCD camera (SITe, 16 bit dynamic range, time integrated) with 0.006-mrad resolution in the Schmidt configuration (optical aperture of 1.34 m, FOV 0.6° full angle, 30 times the laser beam diameter).

Spectral measurements of the backscattered light have been performed with the same telescope in a Coudé configuration with 1.2-arcsec full aperture and an apparent aperture number of $f/46$. The signal was analyzed with an Echelle spectrograph[39] with a dispersion of 0.042–0.073 Å per 15 μm CCD pixel (EEV limited, 16-bit dynamic range, time integrated) in the spectral range of interest (538–927 nm). The instrument-broadening function has been measured to be Gaussian, with a typical resolution of 0.1 Å (0.1 cm^{-1}). The signal was averaged over several minutes (3000 to 12,000 laser shots at 10 Hz). All measurements were correlated with the results of an auxiliary, classical lidar detection providing real-time measurement of the height and thickness of the clouds.

3. PARTICLE SIZE DISTRIBUTION FROM MULTIPLE-SCATTERING PATTERN

Cloud characterization requires the measurement of the droplet size distribution and number density. Recent experiments have shown that clouds or aerosol layers located at an altitude of several kilometers yield valuable signals when backscattered photons[37] are imaged (Fig. 1). Such images bear two types of information. On the one hand, differentiating the beam diameter as a function of altitude below the cloud (see arrow in Fig. 1) yields the beam divergence, which amounts to 0.16 mrad in the fundamental wavelength.[37] On the other hand, the wide-scattering halo on the cloud is a clear signature for strong multiple scattering within it. Once corrected with the parallax induced by the experimental configuration, a cut across this halo provides us with the angular pattern of the multiple scattering, bearing information about the cloud itself. Since the ionization of self-guided filaments generated by high-intensity femtosecond lasers have been shown to trigger condensation in supersaturated atmospheres,[31] we ascertained that no filamentation occurred at the cloud altitude, in order to avoid affecting the droplet formation.

High-resolution images of the pattern around 800 nm provide for the first time a multi-FOV[5–8] lidar at this an-

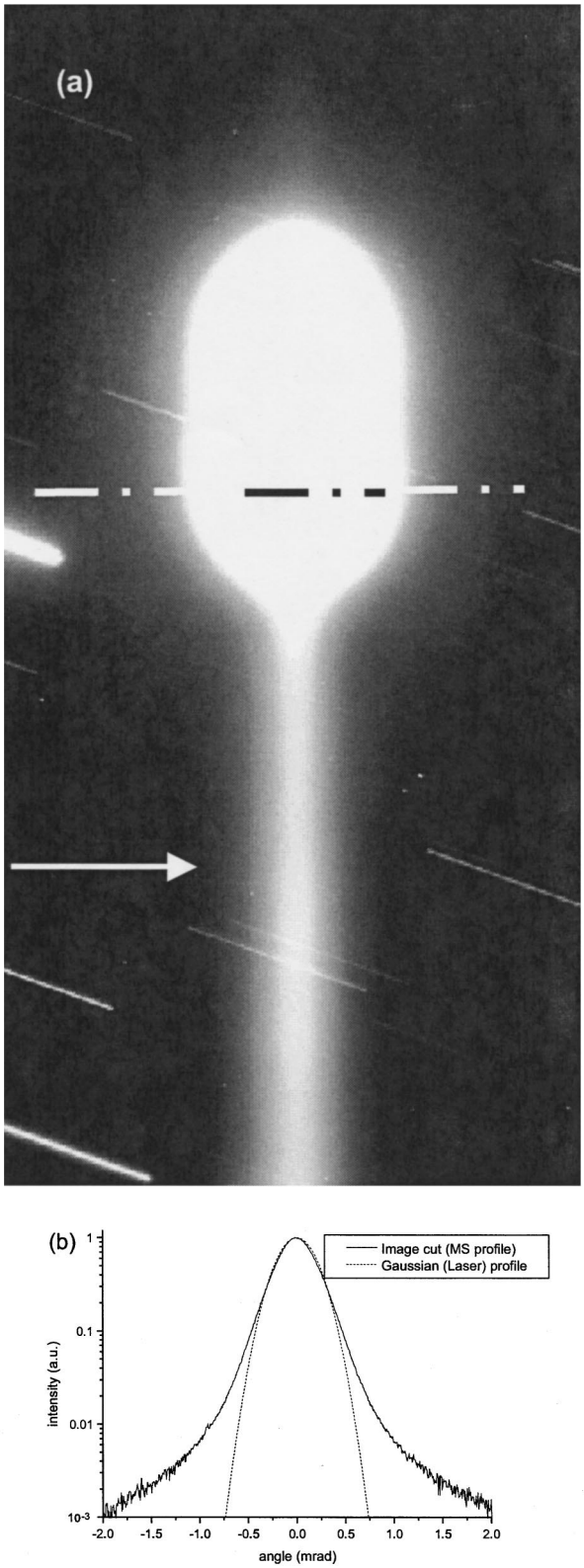

Fig. 1. (a) Beam image observed from the ground in a spectral band near the fundamental wavelength (800 nm). The lower part of the image (see arrow) corresponds to Rayleigh scattering of the beam below the cloud. The halo is due to multiple scattering in the cloud at 6-km altitude. (b) Multiple scattering patterns obtained by geometry-corrected cuts across the halo (see dotted line), and Gaussian profile corresponding to the laser beam. The difference between the two profiles stems from multiple scattering.

gular resolution, which allowed us to fit the droplet size distribution within the cloud using a genetic algorithm.[40] The particle size distribution was modeled by 18 size classes between 0.1 and 20 μm. The weights of each size class were the free parameters. Since we rely on laser beam images on the cloud, we obtained depth-integrated data, which led us to consider that the size distribution is homogeneous within the cloud depth. To avoid possible slight errors induced by multiple scattering on the measurement of the beam divergence,[37] we also left the exact beam divergence as a free parameter. The genetic algorithm used to determine the size distribution works as follows. A set of 100 "individuals," i.e., temptative solutions (size distribution and laser divergence) was randomly generated, and the corresponding theoretical multiple-scattering patterns were computed, as detailed below. Then the 30 best solutions, i.e., those who fit the experimental pattern better, were selected and combined to form 100 new ("children") temptative solutions, and the algorithm was iterated until convergence was achieved after 580 iterations.

To compute the theoretical multiple-scattering pattern corresponding to a given size distribution, we first averaged the calculated Mie scattering angular pattern over each size class. The use of Mie scattering is supported by temperatures of -25 °C to -20 °C measured at the cloud height (6 km) by radiosondes during the multiple-scattering measurement. This temperature is well above the -35 °C threshold for a full freezing of the water particles, allowing us to consider the particles as spherical droplets. To model a smooth size distribution, we used a Gaussian shape for each class, and the width was chosen so that the wings of neighboring classes slightly overlapped. Then we generated an effective overall angular Mie scattering pattern by averaging the contribution of each size class, weighted according to the temptative solution under consideration. This angular pattern was then used to simulate the multiple-scattering pattern, treating the nth-order scattering as n individual scattering event, with the angular probability given by the effective Mie scattering pattern of the size distribution.[41] Between the scattering events, we considered propagation segments of a length equal to the mean free path of a photon in the cloud $L_{\mathrm{mfp}} = 1/[2\pi\Sigma N_i r_i^2 Q_s(r_i)]$, where N_i is the particle density of class i, r_i is its droplet radius, and $Q_s(r_i)$ is the corresponding scattering coefficient calculated from Mie theory for water droplets with refractive index $n = 1.334$. The auxiliary lidar provided a cloud altitude of 6 km and a thickness of $\sim$1 km, much more than the mean free path of photons within it (10–1000 m for the considered ranges for particle densities and optical thicknesses), so we were able to neglect rays lost by scattering beyond the top of the cloud. Since we deal with relatively dense clouds, Rayleigh scattering from air molecules is neglected. As measured below the cloud, the incident laser beam is considered Gaussian, with a divergence of several tenths of a milliradian.

Tests within the entire parameter range of interest showed that the orders beyond fourth-order scattering had a negligible contribution to the scattering pattern ($<5\%$). Hence, calculations are restricted to the orders 1 (single scattering) through 3 in the following, reducing the computing time and allowing iterative fitting of the experimental pattern. As shown in Figs. 2 and 3, the simulated radial multiple-scattering profile of individual size classes critically depends on the particle size and density within the cloud, allowing to determine the average particle size within the cloud.

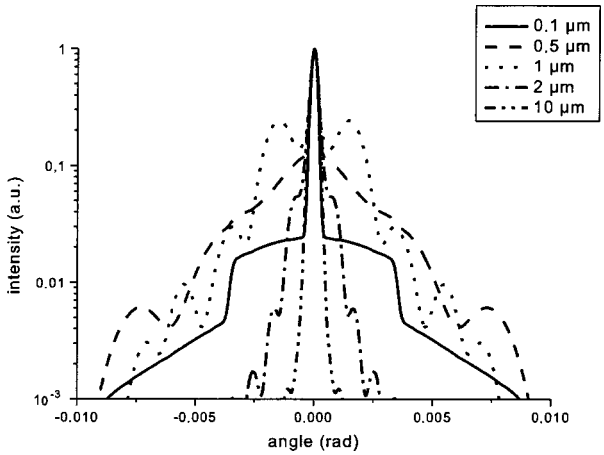

Fig. 2. Simulated angular multiple scattering profiles at 800 nm for monodisperse clouds composed of 0.1-, 0.5-, 1-, 2-, and 10-μm water droplets, with an extinction coefficient of $\alpha = 3.27 \times 10^{-2}\,\mathrm{m}^{-1}$, corresponding to a cloud penetration depth of $\sim$30 m.

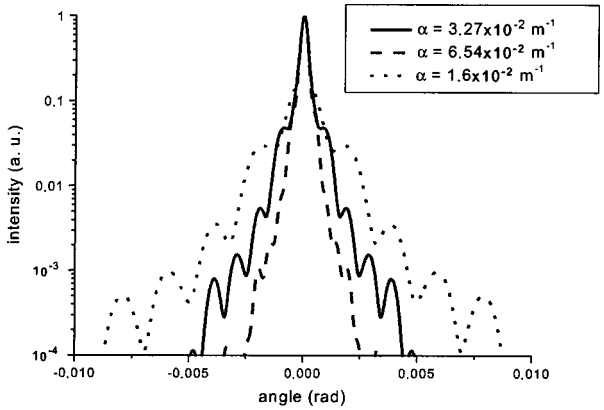

Fig. 3. Simulated angular multiple scattering profiles at 800 nm for monodisperse clouds composed of 2-μm water droplets, as a function of the extinction coefficient α. The corresponding penetration depths are 30, 15 and 60 m.

Figure 4 shows the obtained fitted size distribution. Its maximum is peaked around 5 μm, in line with median values reported in the literature for continental stratus clouds.[42,43] The corresponding mean free math $L_{\mathrm{mfp}} = 700\,\mathrm{m}$ and extinction coefficient $\alpha = 1.4 \times 10^{-3}\,\mathrm{m}^{-1}$ are qualitatively compatible with both the intense signal in the auxiliary lidar detection system and the fact that the auxiliary lidar signal can be received through the 1-km-thick cloud layer.

The droplet size distribution and the cloud density retrieval over more than 15 size classes were made possible by the high-resolution multi-FOV data available from the images of the laser beam on the bottom of the clouds. Moreover, we also recorded similar multi-FOV data in the 400–500 spectral region of the white-light continuum.[37] The simultaneous analysis of the multiple-scattering pat-

terns in two or several spectral regions, with different penetration depths, may provide an opportunity for one to circumvent the intrinsic depth integration of each of our monochromatic data, yielding layered size-distribution data. Independent fits at several wavelengths could also help validate the technique by providing data about the same size distribution.

4. RELATIVE HUMIDITY RETRIEVAL

Besides the droplet size distribution, characterization of the cloud microphysics requires knowledge of the thermodynamical parameters of the atmosphere around it, including relative humidity and temperature. We achieved this measurement with the same laser source as the multiple-scattering study for droplet sizing described in Section 3, thus prouding the potential for a simultaneous measurement.

More precisely, we analyzed the range-integrated spectrum of the white-light continuum backscattered from clouds located 4.5 km above the ground level, as measured by the auxiliary lidar. The cloud is treated as a hard target, neglecting the penetration depth of less than $100\,\mathrm{m} \ll 4.5\,\mathrm{km}$ measured by the auxiliary lidar. The spectrum of the backscattered white light was recorded between 680 and 920 nm,[31] thus encompassing in the same measurement the rotational-vibrational band of H_2O centered at 820 nm, as well as the O_2 A band around 762 nm.

Since the available spectral range covers lines of different intensities, the bands used in the fit have been chosen to optimize the signal while avoiding saturation, in relation to the actual concentration of the species to be measured. Two fitting procedures, both benefitting from the wide available spectral interval, have been applied independently to two spectra acquired under different laser parameters, to crosscheck the results. The fits are based on HITRAN 2000[44] high-resolution database. The instrumental resolution is ten times broader than that required for differential absorption lidar measurements of pressure or temperature profiles by use of water vapor lines or the O_2 A band.[17,45] However, since the fit is performed over a broad spectral range, we were able to convolve each synthetic spectrum with the known instrumental-broadening function in the fitting procedure. The accuracy of this technique was also checked numerically over simulated spectra. The broad spectral range, together with the narrowness of the absorption lines that we considered, permitted us to circumvent the poor characterization of the white-light continuum source and of the backscatter spectral efficiency on the cloud. Since these functions are known to be smooth, we fitted them as a smooth baseline on the recorded spectrum, as is common e. g., in astronomy. Then this baseline is used to normalize the absorption spectrum over the entire spectral range.

The first procedure was applied to a spectrum acquired at 22:00 UT. The temperature was retrieved from the O_2 A band spectrum and subsequently used to fit the water vapor VMR of the atmosphere from water absorption band of the same spectrum. More precisely, the stable meteorological conditions allowed us to consider a stan-

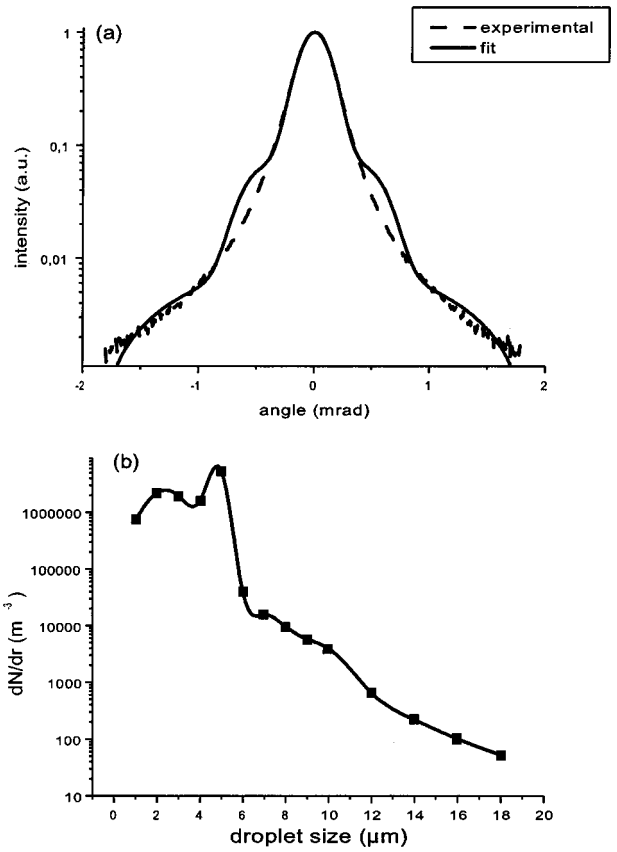

Fig. 4. (a) Experimental and fitted angular distribution of multiple scattering, corresponding to the data of Fig. 1. (b) Corresponding droplet size distribution in the cloud retrieved with the genetic algorithm.

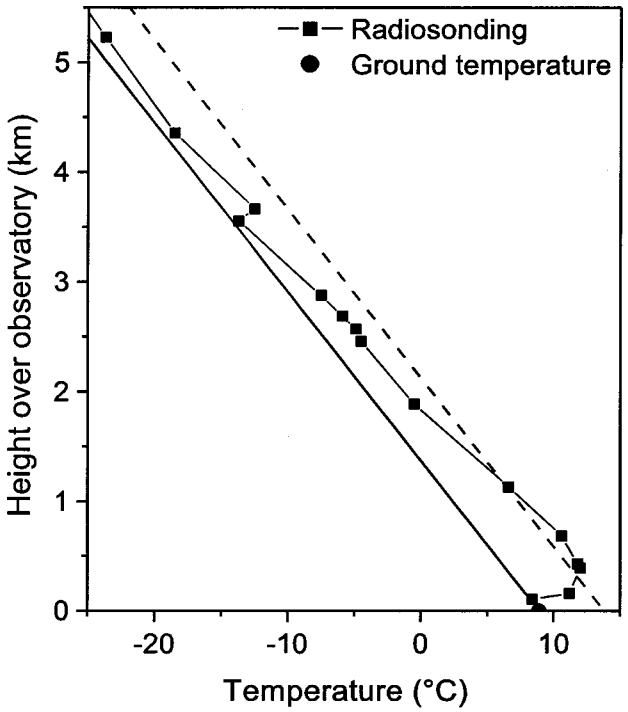

Fig. 5. Temperature determined by a fit of the O_2A band on the white-light absorption spectrum, and the nearest radiosonde data available (Meiningen, 23:00 UT).

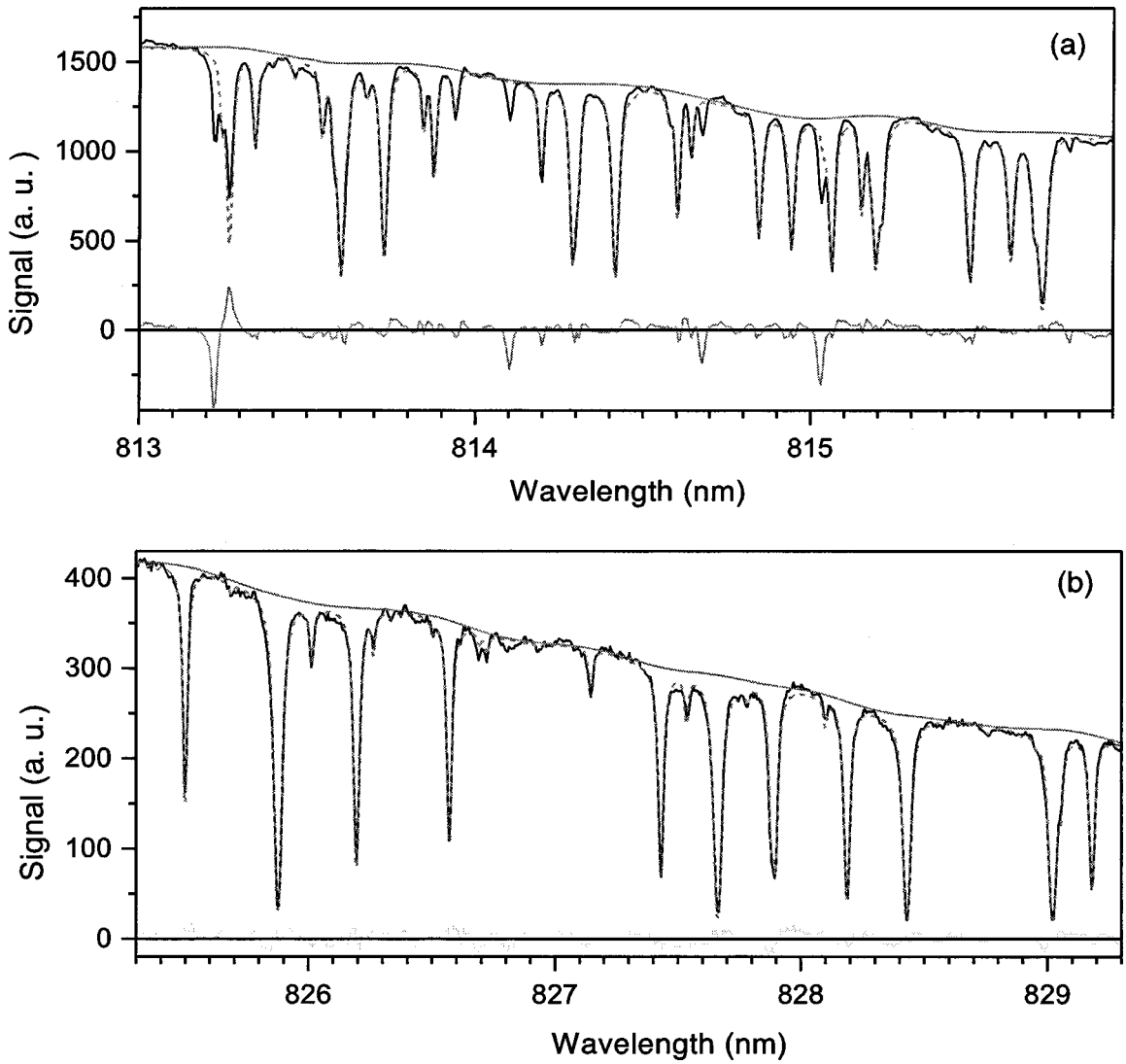

Fig. 6. Fit of the water absorption spectrum in the 4ν-overtone band in the (a) 813–816 nm and (b) 825–829 nm regions. Black solid curve, measurement; gray dotted curve, fit; lower gray solid curve, residuum of the fit. The lower black line is the estimation of the baseline. Note that the extremely long absorption path allows us to measure weak lines not tabulated in the HITRAN 2000 database.

dard vertical pressure profile and a typical temperature decrease by 6.5 K/km (treated with a vertical resolution of 100 m), and the known VMR of oxygen in the atmosphere (20.9%) was considered. The fitting parameters were the ground temperature (T_g) and the emission altitude of the white light (z_{WL}). The filament length is neglected, since we have found that it is much shorter than the absorption length under our experimental conditions.[37] Fits in the 761–764 nm and the 766–769 nm ranges both yield $T_g = 287 \pm 1$ K and $z_{\mathrm{WL}} = 550 \pm 100$ m. Note that the filament altitude obtained for a medium group velocity dispersion precompensation (300 fs initial pulse duration) is in line with data obtained independently with a geometrical method.[37] The ground temperature is slightly higher than measured at ground level during the experiment (282 K). However, the nearest radiosonde temperature profile available (23:00 UT, Meiningen, at 100-km distance, Fig. 5) shows that this discrepancy is due to a sharp temperature gradient near to the ground, below the white-light emission altitude. Therefore the retrieved temperature is reasonable.

This profile and white-light emission altitude were used as references to determine the relative humidity, which was supposed to be constant over the considered altitude range. More precisely, the above-determined temperature and pressure profiles were used to get the relative humidity values from the corresponding water vapor VMR, with the same 100-m resolution. The fit was performed in the water vapor 4ν-overtone band in both the 813–816 nm and the 825–829 nm regions (Fig. 6). This fit yields a relative humidity of $(49 \pm 3)\%$, in good agreement with the vertical average of the radiosonde data (Fig. 7). Hence, white-light lidar data have, for the first time, allowed multicomponent measurements yielding both temperature profile and relative humidity data, which are key parameters in the understanding of the physics of cloud formation and precipitation.

This result was cross checked by a second independent fitting procedure in which both the mean temperature and the water mixing ratio (VMR) of the atmosphere were obtained simultaneously from the same fit of the experimental spectrum over the 815–840 nm spectral region

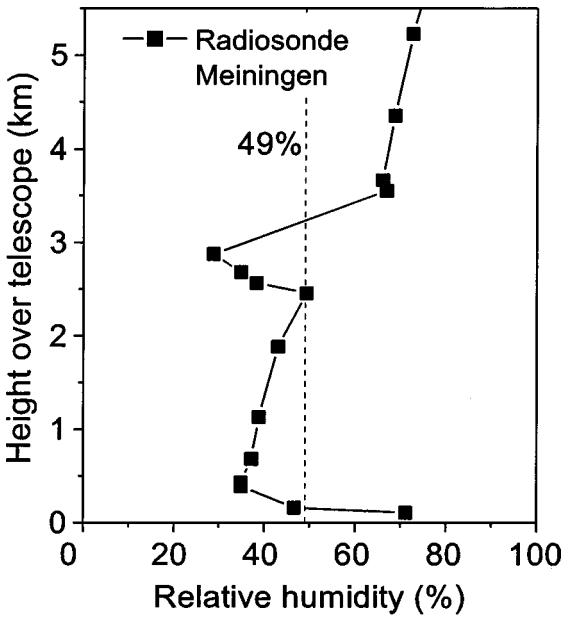

Fig. 7. Retrieved average relative humidity (dotted line) and RH profile measured by radiosonde (solid line). Note that a cloud layer around 3 km at the radiosonde site perturbs the corresponding measurement.

(4ν-overtone band). Here, the filaments are considered to span over a short altitude range near the laser output.[34] Hence, the absorption length of the white light is fixed to 9 km. The fit yields a vertically averaged humidity and temperature of $0.38 \pm 0.01\%$ and 279.2 ± 0.4 K, respectively. The resulting relative humidity at ground level is therefore estimated to be $42 \pm 3\%$, comparable with the result of the first fit.

Spectral measurements thus simultaneously yielded the temperature and the relative humidity of the air mass under the clouds, within an error compatible with the requirements of meteorological or climatological modeling purposes. Two variants have been demonstrated in which multiple parameters are retrieved either from distinct spectral regions or from one single, broad wavelength interval. Since the presented results are range-integrated measurements, the analysis required assumptions about the vertical profile of both water vapor and temperature in the atmosphere. Although these assumptions are validated by radiosonde data in the case of our experiments, in principle deviations from the standard models used will cause errors in the data analysis. However, this range integration and the use of a cloud as a target are not intrinsic to the white-light lidar technique, since the CCD detectors can be time gated. Although Rayleigh backscattering in free atmosphere is 100 to 1000 times less efficient than Mie backscattering from a typical cloud, a better fitting of the telescope field of view with the laser divergence, i.e., 1 mrad instead of 6 μrad, would improve the signal by a factor of 3×10^4. Hence, the signal would still be ten times more intense, allowing us to reduce the integration time by a factor of 10. Then differentiating the backscattered white light with respect to altitude would yield altitude-resolved relative humidity profiles, therefore allowing for humidity mapping across the atmosphere.

5. CONCLUSION

In conclusion, we have shown that a lidar technique using the supercontinuum generated by the filamentation of femtosecond pulses during their vertical propagation in the atmosphere can be used to analyze both the clouds (droplet size distribution and number density) and the thermodynamical properties of the atmosphere in their vicinity, such as the temperature and relative humidity. Since both of these measurements use the same laser source equipped with suitable diagnostics for imaging and spectral analysis, they are suitable for a simultaneous operation. Although preliminary, they open the way to a multiparameter analysis of the cloud microphysics by combined white-light differential absorption and multi-FOV lidar. Routinely obtaining such data about the cloud microphysics would be of high relevance for atmospheric modeling, especially considering the two-dimensional and three-dimensional mapping capability of lidar.

However, the present experiment does not fully use the potential of the described technique. The use of several wavelengths in multi-FOV aerosol analysis would yield more-precise size distributions of the aerosols in the clouds and may even allow us to determine layered size-distribution data. Also, range-resolved spectral measurements using time-gated multichannel detectors would yield relative humidity profiles and release the need for assumptions about the atmospheric temperature and water VMR profiles in the data analysis. Moreover, the practical use of the technique described in this paper, e.g., for routine measurements, requires eye safety, which drastically limits the laser power at 800 nm. However, the white-light lidar measurements are performed at a wavelength that is independent of the laser source. Therefore the currently developing high-power, ultrashort lasers in both the UV and in the telecom window raise the hope of application of the white-light lidar techniques to laser sources in wavelength bands where eye safety can be achieved at much higher powers, compatible with that required for nonlinear effects.

ACKNOWLEDGMENTS

The Teramobile project acknowledges support of the Center National de la Recherche Scientifique (France) and the Deutsche Forschungsgemeinschaft (Germany). The Teramobile members would like to thank the technical staff of the Thüringer Landessternwarte Tautenburg (TLS), Bernd Furhmann, Jürgen Haupt, Axel Kirchhof, Michael Pluto, Jörg Schiller, and Johannes Winkler, for their assistance in installing the laser at TLS and helping to solve technical problems. We also thank Eike Guenther, Sylvio Klose, and Helmut Meusinger for helpful discussions on conducting the observations with the 2-m telescope. The Teramobile web site is www.teramobile.org.

REFERENCES

1. H. R. Pruppacher and J. D. Klett, *Microphysics of Clouds and Precipitation* (Reidel, Dordrecht, The Netherlands, 1978).
2. R. M. Measures, *Laser Remote Sensing—Fundamental and Applications* (Wiley Interscience, New York, 1984).

3. B. Stein, M. Del Guasta, J. Kolenda, M. Morandi, P. Rairoux, L. Stefanutti, J. Wolf, and L. Wöste, "Stratospheric aerosol size distribution from multispectral lidar measurements at Sodankylä during EASOE," Geophys. Res. Lett. **21,** 1311–1314 (1994).
4. D. M. Winker and M. P. McCormick, "Aerosol and cloud sensing with the Lidar In-space Technology Experiment (LITE)," in *Lidar Techniques for Remote Sensing*, C. Weiner, ed., Proc. SPIE **2310**, 98–105 (1994).
5. S. R. Pal and A. I. Carswell, "Multiple scattering in atmospheric clouds: lidar observations," Appl. Opt. **15**, 1990–1995 (1976).
6. J. S. Ryan, S. R. Pal, and A. I. Carswell, "Laser backscattering from dense water-droplet clouds," J. Opt. Soc. Am. **69**, 60–67 (1979).
7. L. R. Bissonnette and D. L. Hutt, "Multiply scattered aerosol lidar returns: inversion method and comparison with in-situ measurements," Appl. Opt. **34**, 6959–6975 (1995).
8. L. R. Bissonnette, "Multiple-scattering lidar equation," Appl. Opt. **35**, 6449–6465 (1996).
9. R. A. Ferrare, E. V. Brownell, S. Ismail, V. G. Brackett, M. B. Clayton, M. Fenn, L. Heilman, S. A. Kooi, D. D. Turner, M. J. Mahoney, R. E. Newell, Y. Zhu, E. Jensen, J. Barrick, and G. Sachse, "Lidar measurements of relative humidity and ice supersaturation in the upper troposphere," presented at the International Laser Radar Conference, Vichy, France, July 10–14, 2000.
10. S. Ismail and E. V. Browell, "Airborne and spaceborne lidar measurements of water vapor profiles: a sensitivity analysis," Appl. Opt. **28**, 3603–3615 (1989).
11. G. Ehret, C. Liemle, W. Renger, and G. Simmet, "Airborne remote sensing of tropospheric water vapor with a near-infrared differential absorption lidar system," Appl. Opt. **32**, 4534–4551 (1993).
12. C. Flamant, J. Pelon, L. Eymard, and J. Tournadre, "SSM/I integrated water vapor content measurements in coastal regions: a comparison with shipborne and airborne remote sensing measurements, radiosonde measurements, and NWP model retrievals," J. Geophys. Res. **108**(C3), FET4-1-20 (2003).
13. L. Garand, E. Gerard, D. Tan, V. Wulfmeyer, G. Ehret, and P. Di Girolamo, "WALES (Water Vapour Lidar Experiment in Space): impact of space borne measurements on NWP and climate research," in *Proceedings of Twenty-First International Laser Radar Conference*, Vol. 2, pp. 755–758.
14. A. Heliere, J. L. Bezy, P. Bensi, and P. Ingmann, "System definition of the ESA Earth Explorer WALES mission," in *Sensors, Systems, and Next-Generation Satellites VI*, H. Fujisada, J. B. Lurie, M. L. Aten, and K. Weber, eds., Proc. SPIE **4881**, 24–32 (2003).
15. A. J. Wimmers, J. L. Moody, E. V. Browell, J. W. Hair, W. B. Grant, C. F. Butler, M. A. Fenn, C. C. Schmidt, J. Li, and B. A. Ridley, "Signatures of tropopause folding in satellite imagery," J. Geophys. Res. **108**(D4), 8360 (2003).
16. D. D. Turner, R. A. Ferrare, L. A. Heilman, and T. P. Tooman, "A two year climatology of water vapor and aerosols in the lower troposphere measured by a Raman lidar," presented at the International Laser Radar Conference, Vichy, France, July 10–14, 2000.
17. J. Bösenberg, "Measurements of the pressure shift of water vapor absorption lines by simultaneous photoacoustic spectroscopy," Appl. Opt. **24**, 3531–3534 (1985).
18. M. Douard, R. Bacis, P. Rambaldi, A. Ross, J.-P. Wolf, G. Fabre, and R. Stringat, "Fourier-transform lidar," Opt. Lett. **20**, 2140–2142 (1995).
19. F. A. Theopold, C. Weitkamp, and W. Michaelis, "Double-cavity étalon in the near infrared," Opt. Lett. **18**, 253–255 (1993).
20. C. R. Philbrick, "Application of Raman lidar advancements in meteorology and air quality monitoring," in *Lidar Remote Sensing for Industry and Environment Monitoring III*, U. N. Singh, T. Itabe, and Z. Liu, eds., Proc. SPIE **4893**, 61–69 (2003).
21. G. Pappalardo, A. Amodeo, S. Amoruso, V. Cuomo, P. Di Girolamo, F. Esposito, L. Leone, L. Mona, M. Pandolfi, G. Pavese, R. Restieri, and C. Serio, "Measurement campaign of atmospheric water vapor and aerosols in southern Italy," in *Optical Remote Sensing of the Atmosphere and Clouds III*, H.-L. Huang, D. Lu, and Y. Sasane, eds., Proc. SPIE **4891**, 353–360 (2003).
22. A. Braun, G. Korn, X. Liu, D. Du, J. Squier, and G. Mourou, "Self-channeling of high-peak-power femtosecond laser pulses in air," Opt. Lett. **20**, 73–75 (1995).
23. E. T. J. Nibbering, P. F. Curley, G. Grillon, B. S. Prade, M. A. Franco, F. Salin, and A. Mysyrowicz, "Conical emission from self-guided femtosecond pulses in air," Opt. Lett. **21**, 62–64 (1996).
24. A. Brodeur, C. Y. Chien, F. A. Ilkov, S. L. Chin, O. G. Kosareva, and V. P. Kandidov, "Moving focus in the propagation of ultrashort laser pulses in air," Opt. Lett. **22**, 304–306 (1997).
25. M. Mlejnek, E. M. Wright, and J. V. Moloney, "Dynamic spatial replenishment of femtosecond pulses propagating in air," Opt. Lett. **23**, 382–384 (1998).
26. N. Aközbek, A. Iwasaki, A. Becker, M. Scalora, S. L. Chin, and C. M. Bowden, "Third-harmonic generation and self-channeling in air using high-power femtosecond laser pulses," Phys. Rev. Lett. **89**, 143901 (2002).
27. G. Méjean, J. Kasparian, J. Yu, S. Frey, E. Salmon, J. P. Wolf, L. Bergé, and S. Skupin, "UV-supercontinuum generated by kilometer-range filamentation in air," Phys. Rev. Lett., submitted for publication.
28. J. Kasparian, R. Sauerbrey, D. Mondelain, S. Niedermeier, J. Yu, J.-P. Wolf, Y.-B. André, M. Franco, B. Prade, S. Tzortzakis, A. Mysyrowicz, M. Rodriguez, H. Wille, and L. Wöste, "Infrared extension of the supercontinuum generated by fs-TW-laser pulses propagating in the atmosphere," Opt. Lett. **25**, 1397–1399 (2000).
29. L. Wöste, C. Wedekind, H. Wille, P. Rairoux, B. Stein, S. Nikolov, Ch. Werner, S. Niedermeier, H. Schillinger, and R. Sauerbrey, "Femtosecond atmospheric lamp," Laser Optoelektron. **29**, 51–53 (1997).
30. P. Rairoux, H. Schillinger, S. Niedermeier, M. Rodriguez, F. Ronneberger, R. Sauerbrey, B. Stein, D. Waite, C. Wedekind, H. Wille, and L. Wöste, "Remote sensing of the atmosphere using ultrashort laser pulses," Appl. Phys. B **71**, 573–580 (2000).
31. J. Kasparian, M. Rodriguez, G. Méjean, J. Yu, E. Salmon, H. Wille, R. Bourayou, S. Frey, Y.-B. André, A. Mysyrowicz, R. Sauerbrey, J.-P. Wolf, and L. Wöste, "White-light filaments for atmospheric analysis," Science **301**, 61–64 (2003).
32. G. Méjean, J. Kasparian, E. Salmon, J. Yu, J.-P. Wolf, R. Bourayou, R. Sauerbrey, M. Rodriguez, L. Wöste, H. Lehmann, B. Stecklum, U. Laux, J. Eislöffel, A. Scholz, and A. P. Hatzes, "Towards a supercontinuum-based infrared lidar," Appl. Phys. B **77**, 357–359 (2003).
33. G. G. Matvienko, V. V. Veretennikov, G. M. Krekov, and M. M. Krekova, "Remote sensing of atmospheric aerosols with a white-light femtosecond lidar," Atmos. Oceanic Opt. **16**, 1013–1019 (2003).
34. H. Wille, M. Rodriguez, J. Kasparian, D. Mondelain, J. Yu, A. Mysyrowicz, R. Sauerbrey, J.-P. Wolf, and L. Wöste, "Teramobile: a mobile femtosecond-terawatt laser and detection system," Eur. Phys. J.: Appl. Phys. **20**, 183–190 (2002).
35. M. C. Galvez, M. Fujita, N. Inoue, R. Moriki, Y. Izawa, and C. Yamanaka, "Three-wavelength backscatter measurement of clouds and aerosols using a white light lidar system," Jpn. J. Appl. Phys. Part 2 **41**, L284–L286 (2002).
36. J. Yu, D. Mondelain, G. Ange, R. Volk, S. Niedermeier, J.-P. Wolf, J. Kasparian, and R. Sauerbrey, "Backward supercontinuum emission from a filament generated by ultrashort laser pulses in air," Opt. Lett. **26**, 533–535 (2001).
37. M. Rodriguez, R. Bourayou, G. Méjean, J. Kasparian, J. Yu, E. Salmon, A. Scholz, B. Stecklum, J. Eislöffel, U. Laux, A. P. Hatzes, R. Sauerbrey, L. Wöste, and J.-P. Wolf, "Kilometer-range non-linear propagation of fs laser pulses," Phys. Rev. E (to be published).
38. H. Lehmann, "The 2m telescope," http://www.tls-tautenburg.de/telesc.html.
39. H. Lehmann, "Coudé Echelle Spectrograph," http://www.tls-tautenburg.de/coude/echelle_spectrograph.html.

40. T. Back and H. Schwefel, "An overview of evolutionary algorithms for parameter optimization," Evol. Comput. **1**, 1–23 (1993).
41. O. B. Toon and T. P. Ackerman, "Algorithms for the calculation of scattering by stratified spheres," Appl. Opt. **20**, 3657–3660 (1981).
42. A. V. Korolev, G. A. Isaac, I. P. Mazin, and H. W. Barker, "Microphysical properties of continental clouds from *in situ* measurements," Q. J. R. Meteorol. Soc. **127**, 2117–2151 (2001).
43. N. L. Miles, J. Verlinde, and E. E. Clothiaux, "Cloud droplet size distributions in low-level stratiform clouds," J. Atmos. Sci. **57**, 295 (2000).
44. L. S. Rothman, A. Barbe, D. C. Benner, L. R. Brown, C. Camy-Peyret, M. R. Carleer, K. Chance, C. Clerbaux, V. Dana, V. M. Devi, A. Fayt, J.-M. Flaud, R. R. Gamache, A. Goldman, D. Jacquemart, K. W. Jucks, W. J. Lafferty, J.-Y. Mandin, S. T. Massie, V. Nemtchinov, D. A. Newnham, A. Perrin, C. P. Rinsland, J. Schroeder, K. M. Smith, M. A. H. Smith, K. Tang, R. A. Toth, J. Vander Auwera, P. Varanasi, and K. Yoshino, "The HITRAN Molecular Spectroscopic Database: Edition of 2000 Including Updates of 2001," J. Quant. Spectrosc. Radiat. Transf. **82**, 5–44 (2003).
45. G. Mégie, "Mesure de la pression et de la température atmosphériques par absorption différentielle lidar: influence de la largeur d'émission laser," Appl. Opt. **19**, 34–43 (1980).